

## POLYMER FIBER PULL OUT EXPERIMENTAL INVESTIGATION

Arturs Macanovskis \*\*, Vitalijs Lūsis \*, Andrejs Krasnikovs \*\*,\*\*

\*\* Riga Technical University  
Institute of Mechanics

E-mail: [artursmacanovskis@inbox.lv](mailto:artursmacanovskis@inbox.lv)

\* Riga Technical University

Concrete mechanics laboratory

E-mail: [Vitalijs.Lusis@rtu.lv](mailto:Vitalijs.Lusis@rtu.lv)

\*\*\* Riga Technical University

Institute of Mechanics and Concrete mechanics laboratory

E-mail: [Krasnikovs.Andrejs@gmail.com](mailto:Krasnikovs.Andrejs@gmail.com)

### ABSTRACT

Advanced polymer fibers are used in structural applications as micro reinforcement in composite materials with a concrete matrix. Comparing to other fibers such as steel, glass, carbon etc., polymer fibers behave visco-elastically or visco-elasto-plastically. Such fibers having moderate starting elastic modulus are characterized by relatively large elastic deformations and pronounced Poisson's effect during stretching. Concrete prisms with dimensions 10x10x40 cm were fabricated, having different amounts of 3 cm long and 0,75 mm in diameter polymer fibers. All prisms were tested under four point bending conditions and loading velocity  $v = 150$  N/s. An elaborated numerical fiberconcrete cracking model was exploited for prism load – deflection mechanical behavior prediction under four point bending conditions. Numerical results were compared with experimental data.

**Key words:** polymer fibers, concrete prisms, pull-out, four point bending

### INTRODUCTION

The need to use high-quality concrete increases every day. An important role among such materials belongs to fiberconcretes - concrete with the addition of different fibers - metal, glass, carbon, polymer and some others. Adding fibers into the concrete matrix causes a situation when the load bearing capacity of the material after cracking of the concrete matrix (appearances of magistral cracks) decreases within acceptable limits or does not decrease at all. In this work, single polymer synthetic fiber pull -out from a concrete matrix is under investigation. A short synthetic polymer fiber is immersed by one end into the concrete matrix at a certain depth and at a certain angle to the direction of the pulling out force. Thereby - the fiber is oriented (has its angle to the direction of the pulling force from the concrete matrix) and has the embedded length in the concrete matrix. Experimental and theoretical data were obtained for the single fiber pull-out phenomena, as well as for the fiberconcrete prisms four point bending.

### CONCRETE COMPRESSIVE STRENGTH EXPERIMENTAL EVALUATION

With the goal to control the class of a concrete used in experiments, 10 samples, having dimensions of 10x10x10 cm of a concrete without fibers, were prepared and tested under compression loading conditions. Samples were elaborated and were

matured for 28 days and afterwards were tested using the testing machine Controls AUTOMAX System V1.04. Average samples compressive strength was equal to 72 MPa.



**Figure 1.** The sample is centered in the testing machine for compression test

### SINGLE POLYMER FIBER PULL-OUT EXPERIMENTAL INVESTIGATION

A single polymer synthetic fiber (Fig. 2.) was placed in a concrete matrix (Fig. 3) and was oriented at an angle to the future stretching direction. Each fiber was embedded at a specific depth (less or equal to fibers half-length)

corresponding to the accepted experimental program (Fig. 4). Specimens were prepared in the following sequence: Step 1: Were prepared a concrete mix. In the concrete mix, used in experiments a relatively small amount of water was added.

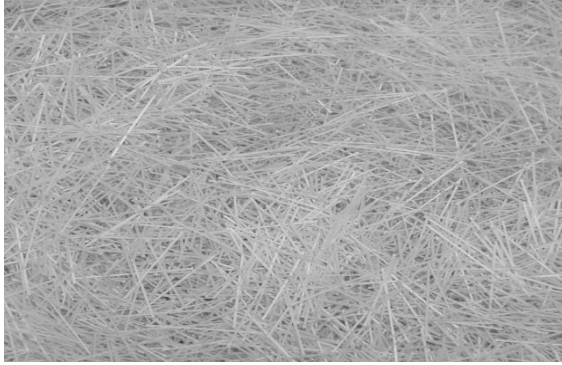


**Figure 2.** Polymer synthetic fibers with the length equal to 3 cm and with the diameter equal to 0.75 mm



**Figure 3.** Samples view for pull-out tests. Is shown how were oriented single fibers in the concrete matrix corresponding to future stretching direction

Step 2: Polymer synthetic fiber is placed into the concrete matrix. Specimen mould was poured in four steps (layers) (Fig. 5).

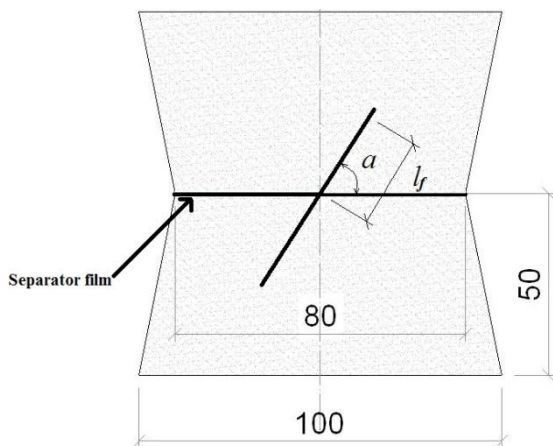


**Figure 4.** A) Configuration of a pull-out test specimen:  $l_f$  - embedded length,  $\alpha$  – inclination angle

The first and second layers were poured into the mould and were well compacted. Layers were rammed carefully with the goal to avoid air bubbles and voids in the concrete. The first and second layers were poured in the form filling exactly half of the depth of a form, in order to facilitate future

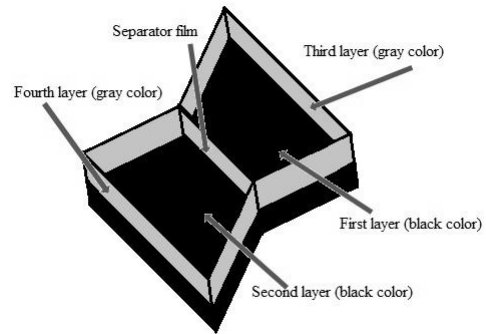


**Figure 5.** Mould filling sequence in the pull-out experiment

fiber emplacement (and orientation) in the mould. Both geometrically similar parts of the sample were separated by a plastic film. Then, after placing the oriented polymer fiber a third layer was poured into one half of the sample mould. The third layer was placed in such way: the concrete mix was taken and superimposed on the fiber, thereby fixing its position and orientation and then the concrete in the form was compacted. Ramming is important otherwise after aging due to macro and micro cavities between fiber and concrete matrix, the polymer fiber without resistance will be pulled out of the concrete. Then the 4th layer was poured. Step 3: Aged specimens experimentally were tested using the tensile testing machine Zwick Roell Z150



**Figure 6.** Sample with fiber oriented under the angle (particular sample shown in the picture has an angle  $60^\circ$ ) to the tension direction

with an additional 1kN load sensor (Fig. 6). Each specimen was placed into the grips and was carefully centered. Two stickers (each with a black horizontal line) were glued on the specimen's both parts, in order to determine their mutual displacement increase, using the noncontact extensometer (camera) MESSPHYSIK (extensometer allows to fix displacement in a thousandth part of a millimeter).

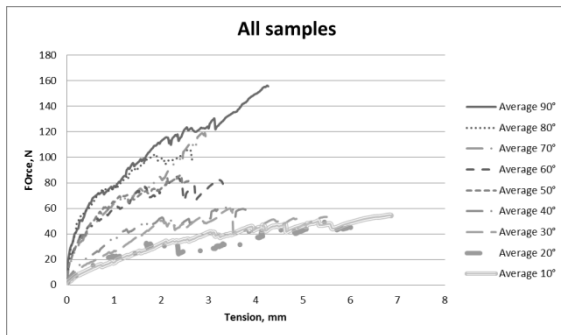


**Figure 7.** Pull-out curves for a polymer synthetic fiber embedded into a concrete under different angles

Fig. 7 shows the applied pulling force- pulled out displacement curves for the polymer macro synthetic fiber which is embedded into the concrete at different angles to the direction of the pulling out force. Each curve was obtained averaging results over eight to ten tested samples.

Pull-out process observation shown two different scenario of fiber pull-out, depended on the angle between the fiber and the stretching direction:

a) if an angle is small ( $10^{\circ}$  -  $20^{\circ}$ ) fiber release in crack zone is happening by concrete matrix spalling and fiber's middle part rotation according to embedment points in both crack flanks. Such oriented fibers can easily break down the concrete matrix and the release of the fiber due to the spalling of the concrete matrix adds to the length which is pulled out of the concrete. Fiber pull-out process starts when distance between crack flanks is reaching few millimeters; b) for fibers oriented under angles from  $30^{\circ}$  to  $90^{\circ}$  fiber that is pulled out of the concrete breaks at a certain depth and the detached end is pulled out by friction which is possible to see in figure 8. For fibers that were oriented under an angle  $90^{\circ}$  it was about 4.5 mm (averaged value over tested fibers were oriented at such angle) and was longer than for fibers oriented under the angles from  $80^{\circ}$  to  $40^{\circ}$ , that was probably caused by the fact that the fibers oriented at angles of  $40^{\circ}$  -  $80^{\circ}$  during pulling out are subjected to cutting shear stresses (spalling of the concrete in the output of the fiber out of concrete only shifts crosssection in which the fiber is subjected to shear).

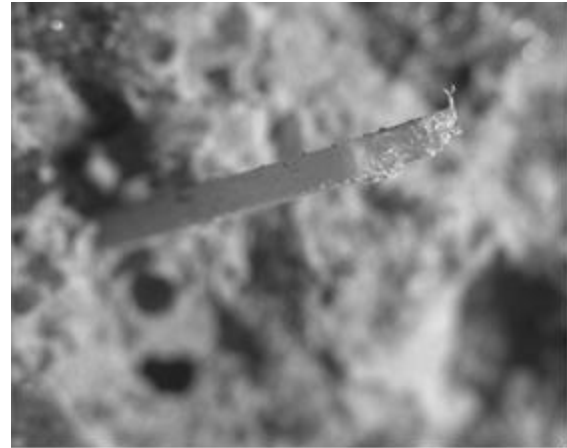


**Figure 8.** Macro synthetic fiber torn out from the concrete (under a microscope)

#### ELABORATION OF FIBERCONCRETE SAMPLES WITH HOMOGENEOUS POLYMER MICRO AND MACRO SYNTHETIC FIBERS SPATIAL DISTRIBUTION

Experimentally samples were elaborated (prisms having dimensions  $100 \times 100 \times 400$  mm) with different fiber concentrations in the concrete matrix. Polymers macro synthetic fibers (Fig. 2) and micro synthetic fibers (Fig. 9) were homogeneously distributed in the material volume.



**Figure 9.** Polymeric micro synthetic fibers (fiber length  $\approx$  5-6 mm, diameter  $\approx$  1mm)

Samples were possible to subdivide into following groups (Fig. 10):

- fiberconcrete samples with micro synthetic fibers;
- fiberconcrete samples with macro synthetic fibers;



**Figure 10.** Samples tested for four point bending

c) fiberconcrete samples with micro and macro synthetic fibers.

Fiberconcrete with micro synthetic fibers was created in follow way:

- 1) all concrete ingredients, without micro synthetic fibers were mixed;
- 2) micro synthetic fibers were added to the concrete. Specimens were prepared with fiber concentrations:  $1\text{kg}/1\text{m}^3$ ,  $2\text{kg}/1\text{m}^3$  and  $3\text{kg}/1\text{m}^3$ .

Fiberconcrete with macro synthetic fibers was created in the following way:

- 1) all concrete ingredients, without macro synthetic fibers were mixed;
- 2) macro synthetic fibers were added to concrete. Specimens were created with concentrations of fibers:  $1\text{kg}/1\text{m}^3$ ,  $2\text{kg}/1\text{m}^3$ ,  $3\text{kg}/1\text{m}^3$ ,  $5\text{kg}/1\text{m}^3$ ,  $6\text{kg}/1\text{m}^3$  and  $8\text{kg}/1\text{m}^3$ .

Fiberconcrete with micro and macro synthetic fibers was created in following way:

- 1) all concrete ingredients, without micro and macro synthetic fibers were mixed;
- 2) in the second step, gradually micro synthetic fibers were added into the mix and then the macro synthetic fibers added. Specimens were created with fibers concentrations of:  $1\text{kg}/1\text{m}^3$  micro and  $1\text{kg}/1\text{m}^3$  macro;  $2\text{kg}/1\text{m}^3$  micro and  $5\text{kg}/1\text{m}^3$  macro;  $2\text{kg}/1\text{m}^3$  micro and  $5\text{kg}/1\text{m}^3$  macro;  $4\text{kg}/1\text{m}^3$  micro and  $4\text{kg}/1\text{m}^3$  macro;  $5\text{kg}/1\text{m}^3$  micro and  $4\text{kg}/1\text{m}^3$  macro;  $8\text{kg}/1\text{m}^3$  micro and  $3\text{kg}/1\text{m}^3$  macro synthetic fibers.

All the samples obtained after complete solidification (28 days) were subjected to experimental testing by four points bending using the tensile testing machine AUTOMAX Controls System V1.04 (Fig. 11).

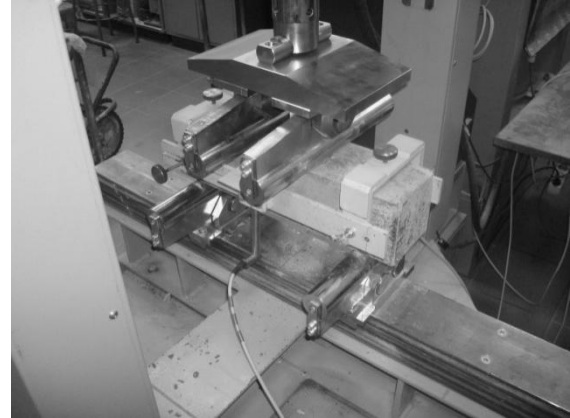


**Figure 11.** Fiberconcrete prism with macro synthetic polymer fibers (concentration –  $8\text{kg}/1\text{m}^3$ ) test by four point bending

#### EXPERIMENTALLY OBTAINED POLYMER MACRO SYNTHETIC FIBERS DISTRIBUTIONS (ACCORDING TO PULL-OUT LENGTH AND ANGLE TO CRACK'S PLANE)

Experimentally distribution of macro synthetic fibers on the crack surface was studied according to location. During the bending test each sample was separated into two pieces. Each sample's both cracked halves surfaces were covered by graphic mesh (mesh cell size  $1\text{cm} \times 1\text{cm}$ ). On both surfaces of the crack location, all of the pulled out macro synthetic fibers were recognized (Fig. 13 and Fig. 14). In table 1 and 2 show every particular fiber crossing of the crack pulled out length and angle to the crack surface plane.

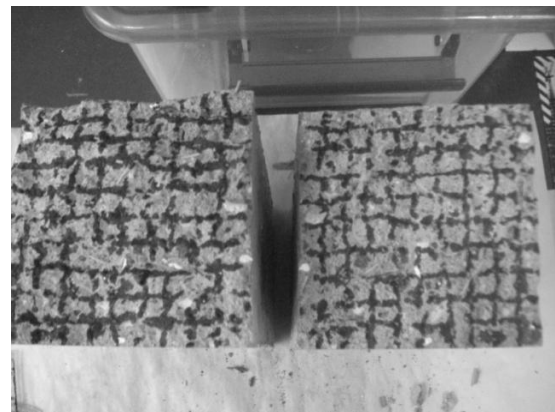


**Figure 12.** View of the grid on one broken sample both parts (concentration of macro synthetic fibers -  $6\text{kg}/1\text{m}^3$ )

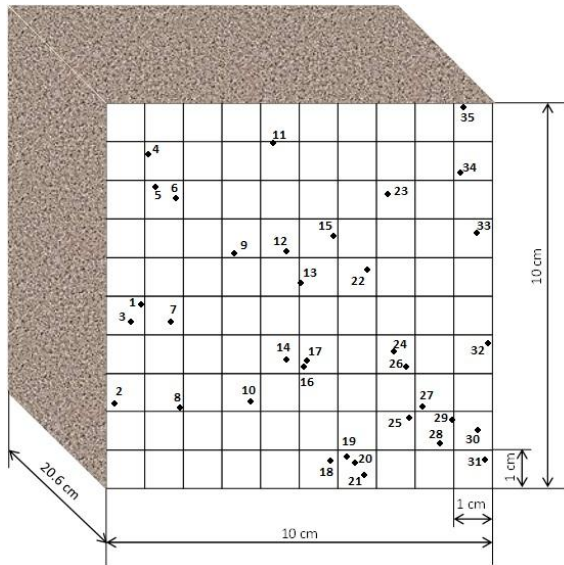


**Figure 13.** Experimental macro synthetic fibers distributions (according to the pulled out length and fiber angle to crack surface) counted on first (left side) crack's side in sample N3. The concentration of fibers in the concrete matrix is  $6\text{kg}/\text{m}^3$

**Table 1**

Experimental macro synthetic fibers distributions (according to the pulled out length and fiber angle to the crack surface) counted on the first (left side) of the crack's side in sample N3

Sample		N3
Number	Angle, °	Length, mm
1	70	4
2	70	10
3	18	13
4	60	9
5	42	5
6	78	4
7	82	5
8	40	8
9	36	4
10	42	5
11	63	7
12	36	12
13	46	6
14	26	9
15	25	7
16	57	2
17	90	4
18	54	3
19	76	8
20	53	7
21	47	5
22	45	9
23	25	10
24	42	5
25	73	5
26	57	7
27	78	5
28	65	8
29	70	4

30	47	5
31	87	13
32	79	14
33	58	8
34	45	3
35	65	9

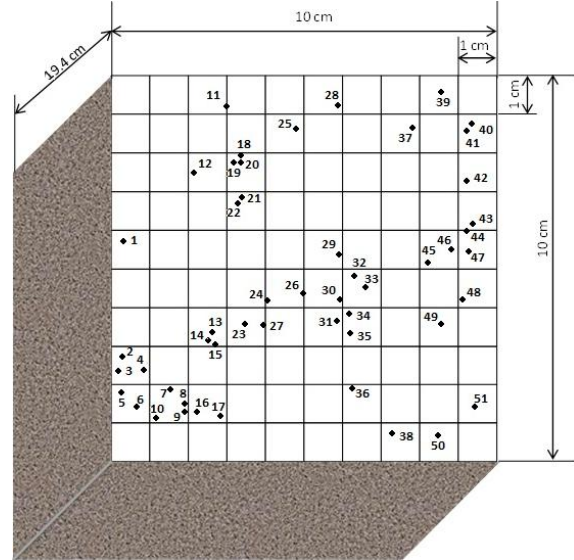


**Figure 14.** Experimental macro synthetic fibers distributions (according to the pulled out length and fiber angle to crack surface) counted on the second (right side) crack's side in sample N3. The concentration of fibers in the concrete matrix is  $6\text{kg}/\text{m}^3$

**Table 2**

Experimental macro synthetic fibers distributions (according to the pulled out length and fiber angle to crack surface) counted on the second (right side) of the crack's side in sample N3

Sample		N3
Number	Angle, °	Length, mm
1	82	8
2	90	4
3	85	17
4	50	6
5	80	9
6	78	6
7	50	7
8	64	10
9	69	7
10	62	4
11	66	4
12	90	2
13	61	10
14	53	9
15	19	15
16	66	4
17	40	10
18	78	6
19	62	4
20	17	7
21	54	5

22	52	3
23	37	4
24	81	4
25	90	7
26	55	3
27	90	2
28	65	2
29	54	2
30	90	7
31	58	6
32	42	6
33	51	3
34	45	6
35	60	5
36	17	16
37	50	6
38	70	2
39	62	5
40	63	7
41	73	4
42	72	4
43	54	8
44	52	10
45	90	2
46	74	3
47	45	3
48	64	2
49	70	6
50	50	6
51	19	4

Following graphics were made:

- The distribution of macro synthetic fibers (crossing the macro-crack) according to angles between the fiber and crack plane (Fig. 15);
- The distribution of macro synthetic fibers on crack surface according to the pulled out ends' lengths (Fig. 16).

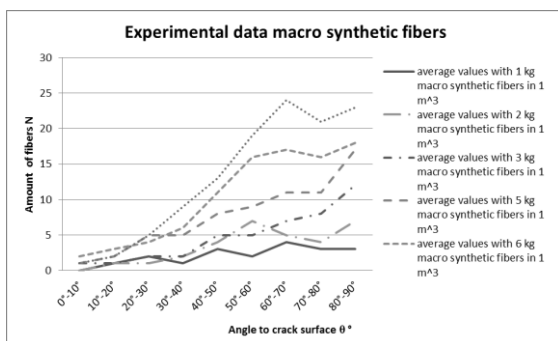


**Figure 15.** Angles to crack surface distribution for pulled out macro synthetic fibers' ends

Looking at figure 15. It is possible to see that those fibers' orientation which are crossing the macro-crack to the crack's plane is non-uniform in all spatial directions. The main reasons for Such phenomena may be two: a) fibers are located under an angle to the pulling out force are obtaining a "quazi" plastical deformation during pulling out;

b) fibers obtained orientation along each prism longitudinal direction when the mould is filled with fresh fiberconcrete. Figure 16 shows that among the pulled out fibers ends, the dominate length is less than 5 mm.

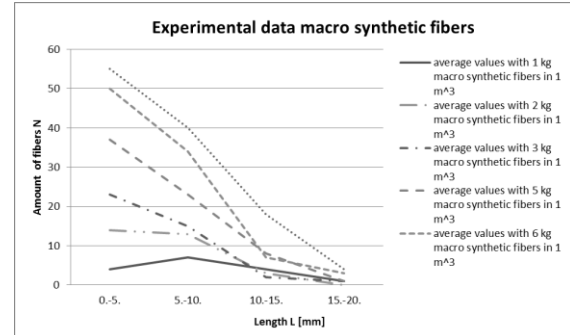


**Figure 16.** Macro synthetic fibers ends distribution according to pulled out lengths

## FIBERCONCRETE SAMPLES LOAD BEARING CAPACITY

Applied force-deflection graphs of the middle of the prism (for material containing micro synthetic fibers), loaded under four point bending conditions, are shown in figure 17. In the figure it is possible to see how the applied force and deflection are increasing, depending on the increasing amount of micro synthetic fibers per 1 m<sup>3</sup>. Samples contained micro synthetic fibers in a range from 1 kg to 3 kg per 1 m<sup>3</sup>. The highest bearing load and maximal deflection ( $\approx 0.052$  mm) was obtained for the highest amount of fibers. Reaching the highest deflection, each prism broke the "quazi" brittle way, separating in two

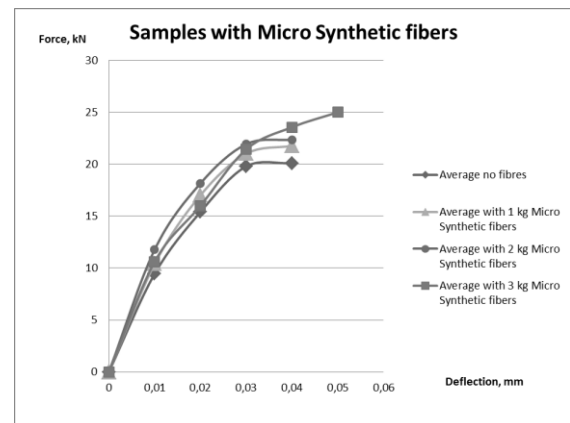


**Figure 17.** Averaged force curves - the vertical deflection of the middle fiberconcrete prisms with micro synthetic fibers when testing on four point bending

parts. Since the micro synthetic fiber is relatively short and small in diameter, the number of such fibers in the material is much higher compared with the concrete containing the same concentration of

macro synthetic fibers. At the same time, the length of pulled out fibers ends of micro synthetic fibers is much shorter than for macro synthetic fibers. Visual view (using a microscope) of the crack's surface is shown in figure 18.



**Figure 18.** Micro synthetic fibers on a macro-crack surface

In figure 19, experimental data obtained in the four point bending tests of fiberconcrete samples are plotted - where macro synthetic fibers are contained. Graphs have two stages at the part corresponding to macro-crack opening (graph's part at which the entire load is carried by stretching and pulling out fibers). Stage 1 – macro- crack cuts a major part of the sample prizm crosssection, the prizm shows a sharp decrease of bearing capacity, this is explained by the fact that the macro synthetic fiber has a low modulus of elasticity and only fibers are carrig lthe oad. Stage 2 – Repeated increase of the load carrying capacity is explained by the fact that the macro synthetic fibers are stretched and after that break in the concrete, the elasto-plastic deformation of the fibers themselves, maintain the highest load.

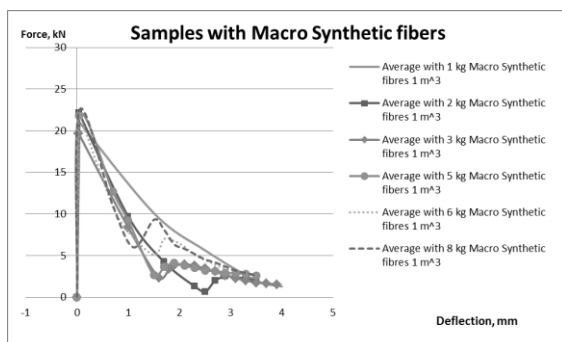


**Figure 19.** The average values of fiberconcrete with macro synthetic fibers after testing on four point bending

In fig. 20 - graphs of the experimental data for fiberconcrete with micro and macro synthetic fibers

that were tested under four point bending conditions are displayed. Adding micro and macro synthetic fibers in concrete, leads to an increase in carrying capacity of fiberconcrete, increase of strength, at the same time, two stages of destruction still remain, as was previously discussed for the graphs in fig.19.

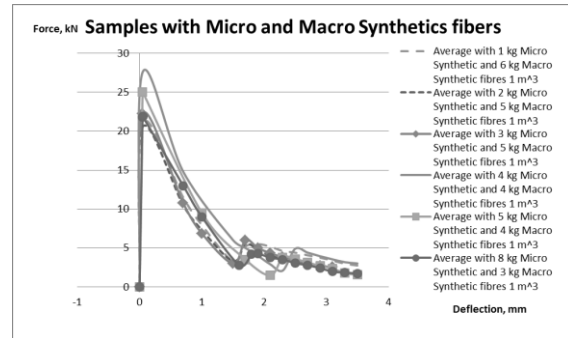


**Figure 20.** The average values fiberconcrete with micro and macro synthetic fibers after testing on four point bending

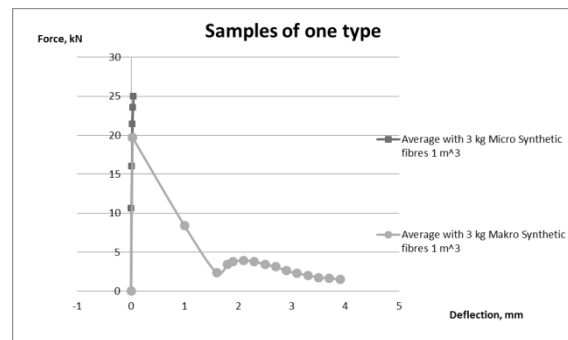


**Figure 21.** The average values of the same type fiberconcrete after testing on four point bending

Figure 21 shows the results of testing for one prism with micro synthetic fibers and one prism with macro- synthetic fibers. It is easy to see that the micro - synthetic fibers are working in fiber cocktails only at the starting stage of rupture. At the same time increase of the material's integrity leads to a higher load bearing capacity of fiberconcrete with a fiber cocktail comparing with material having the same amount of macro- synthetic fibers only.

### THE THEORETICAL MODEL FOR POLYMER FIBER CONCRETE CRACKING N 4 POINT BENDING TESTS

Experimentally obtained pull-out observations were used as the main input data for the numerical model with the goal to predict the linear and non-linear behavior of fiberconcrete beams under bending loads. Because the fibers during being were pulled out of the concrete matrix the ability of the FRC beam to carry applied load in the post-cracking state purely depends on the capacity of fibers in broken crosssection to carry pull-out loads. In the model the

behavior of fiberconcrete beam was simulated by calculating internally existing load bearing value of each fiber crossing the crack (using this fiber experimentally measured pull-out curve), depending on crack opening value  $b_i$  at the location of this particular fiber. The iteration procedure of beam behavior modeling in bending was performed according to step sequence. Further, number of fibers on one crack's surface unit was used as was obtained in experiment. Relation of externally applied load  $P$  as a function of crack opening displacement  $b_i$  is thus obtained at each step. The force  $P$  represents total force applied to the beam that is divided in two symmetrical forces. To run the algorithms of the model, computer software was elaborated. In figure 22:  $\delta_i$  - is the current crack opening at the bottom side of the beam (is called crack mouth opening displacement CMOD). In the same figure  $b(y)$  - is the local opening of the crack at distance  $y$  in crack depth direction from the bottom beam surface.

Since the local opening of crack  $b(y)$  is not constant and varies along the height of the crack the bridging force must be dependent on the local crack opening. In our model, we know all fibers coordinates on the macro-crack surface and every particular fiber orientation angle to crack surface and each fiber shortest end embedded length, as well as how far it is pulled out if CMOD is equal  $\delta$ .

#### ACKNOWLEDGMENT



This work has been supported by the European Social Fund within the project «Support for the implementation of doctoral studies at Riga Technical University».

#### REFERENCES

1. ShaoY., Li Z. and Shan S. (1993) *Journ. Adv. Cem. Based Materials*, 1,p. 55-66.
2. Li V.C. and Chan Y. W. (1994) *ASCE J. Eng. Mech.*, 120, p.707-719.
3. Krasnikovs A., Khabaz A., Telnova I., Machanovsky A. and Klavinsh I. (2010) Numerical 3D investigation of non-metallic (glass, carbon) fiber pull-out micromechanics (in concrete matrix), *Sc. Proceedings of Riga Technical University*, Transport and engineering, 6, vol.33, p.103-108
4. Lapsa V., Krasnikovs A., Eiduks M., Pupurs A. "Method for production the oriented fiberconcrete structures". LV 13929 B. 20.07.2010.

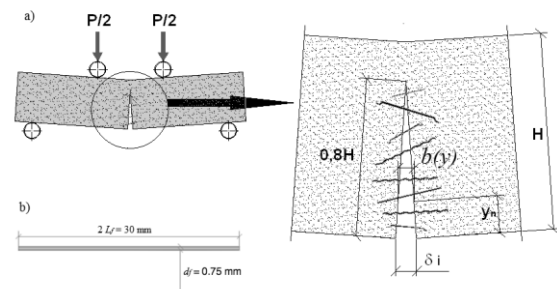


**Figure 22.** a) Schematic representation of beam loads bearing mechanisms during macro-crack opening. Maximal crack opening  $\delta$ = CMOD and local opening of crack  $b(y)$  (at depth  $y$ ). b) Polymer macro synthetic fibers under investigation – straight form

#### CONCLUSIONS

Detailed experimental and numerical fiberconcrete strength and post cracking behavior investigation was performed for material with macro and micro synthetic polymer fibers. Broad experimental program for macro- synthetic fibers pull out of concrete was realized. Peculiarities of fracture for such materials were investigated. Beams with uniformly distributed macro- synthetic fibers, micro- synthetic fibers and simultaneously with macro and micro- synthetic fibers were tested and their mechanical behavior under bending loading conditions was numerically simulated. Numerical modeling results were compared with experiments and recommendations were done.